Journal of Sound and Vibration (1998) **218**(4), 605–618
Article No. sv981855

CONTROL OF SOUND TRANSMISSION THROUGH THIN PLATE

C.-C. Sung and C.-Y. Chiu

National Taiwan University,
Department of Naval Architecture and Ocean Engineering, 73 *Chow-Shan Road*,
Taipei, *Taiwan*, *R.O.C.*

(*Received* 20 *February* 1997, *and in final form* 29 *June* 1998)

Active suppression of the acoustic transmission through plate structure is the major target of this paper. The model consists of a plane acoustic wave incident onto a clamped elastic rectangular thin plate and the piezoceramic patches modelled as four point moments are bonded on the surface of the plate as controllers. Control methods are model based, and rely on state or output feedback to change dynamic characteristic of the plate. The transmitted sound power before and after control is compared using different numbers of controllers. The results show that both the plate responses and the transmission of sound power obtained theoretically and experimentally match. After control the transmitted acoustic power is reduced by about 30–40 dB by one or two piezoelectric ceramics and the global sound pressure level is reduced by about 20–30 dB for low to mid-range frequencies.

1. INTRODUCTION

The interest in sound radiation or transmission control of elastic structure has been increasing in acoustic engineering. Recent research suggests that for structurally radiated noise there is some advantage in applying the control action directly to the structure in the form of vibration inputs. Fuller [1, 2] demonstrated, both experimentally and analytically, that significant reduction in far-field radiated pressure was possible by applying control forces directly to a plate. The experimental work by Fuller used acoustic pressure sensors in the far field to generate a radiated power cost function minimized by using electrodynamic actuators on a circular plate. Akishita [3] used piezoelectric ceramics as actuators and sensors to control sound transmission through a clamped rectangular plate. Optimal use of the piezoelectric ceramic actuator was investigated theoretically by using the transfer function from incident sound pressure to radiated sound pressure.

In this paper, we used piezoelectric ceramics as controllers to suppress the acoustic transmission power for clamped rectangular plate. A piezoelectric ceramic actuator is very attractive because it retains the benefit of compactness and it does not need supporting structure, which can bear reacting force. The model consists

0022–460X/98/490605 + 14 $30.00/0

of a baffled clamped square elastic plate which is excited on one side by a plane acoustic wave as a noise input. The sound field radiated from the other side of the plate, i.e., the transmitted field, was reduced by applying vibrating control forces to minimize the radiated sound power. Active control techniques are modal based and rely on state or output feedback to change dynamic characteristic of the plate. Instead of microphones, we choose accelerometers as error sensors. Since the error sensors will not measure acoustic pressure which is the quantity to be reduced, the present work is concerned with estimating the total radiated power measured on the structure. Using this estimate as a cost function, we design a feedback controller to minimize the cost.

2. GENERAL THEORY

2.1. PLATE RESPONSE

The bending of the thin plate is governed by the following equation when the coordinate system are defined as shown in Figure 1.

$$D\left(\frac{\partial^4}{\partial x^4} + 2\frac{\partial^4}{\partial x^2\,\partial y^2} + \frac{\partial^4}{\partial y^4}\right)w(x, y, t) + \rho_s h\frac{\partial^2 w(x, y, t)}{\partial t^2} = p_e(x, y, t) \qquad (1)$$

where w is the panel displacement, D is the bending stiffness defined by the relation $D = Eh^3/12(1 - v^2)$, E is the modules of elasticity, v is Poisson's ratio, h is the thickness of the plate, ρ_s is the density of the plate and p_e represents the external excitation. Assuming the plate is clamped at four edges, the boundary conditions can be described as follows:

$$w = 0, \qquad \frac{\partial w}{\partial x} = 0 \qquad x = -\frac{a}{2}, \frac{a}{2} \qquad (2)$$

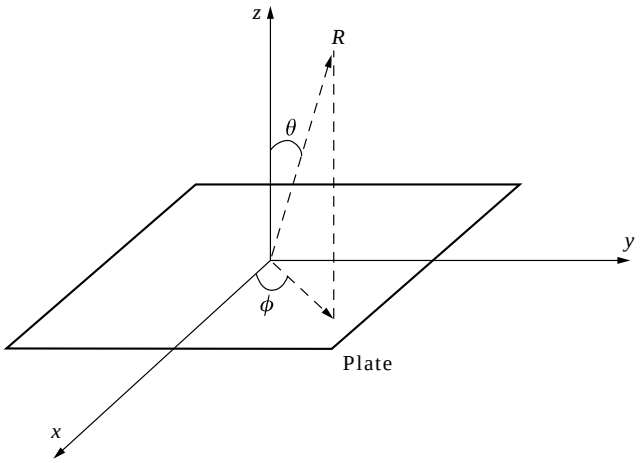

Figure 1. The coordinate system of the plate.

$$w = 0, \qquad \frac{\partial w}{\partial y} = 0 \qquad y = -\frac{b}{2}, \frac{b}{2} \tag{3}$$

where a and b are the length and width respectively.

Through shape functions of the clamped beam [4], the panel displacement $w(\sigma, t)$ can be expressed in terms of a mode shape matrix $S_P(\sigma) = [S_1(\sigma), S_2(\sigma), \ldots, S_l(\sigma)]^{\mathrm{T}}_{1\times l}$ and a modal amplitude matrix $W_P = [W_1, W_2, \ldots, W_l]^{\mathrm{T}}_{1\times l}$ as

$$w(\sigma, t) = S_P(\sigma)^{\mathrm{T}} W_P(t) \tag{4}$$

where $S_l(\sigma) = X_m(x) Y_n(y)$,

$$X_m(x) = J\left(\frac{\lambda_m(x)}{a}\right) - \frac{J(\lambda_m)}{H(\lambda_m)} H\left(\frac{\lambda_m(x)}{a}\right),$$

$$Y_n(y) = J\left(\frac{\lambda_n(y)}{b}\right) - \frac{J(\lambda_n)}{H(\lambda_n)} H\left(\frac{\lambda_n(y)}{b}\right),$$

$$\begin{cases} J(u) = \cosh(u) - \cos(u) \\ H(u) = \sinh(u) - \sin(u)' \end{cases}$$

λ_m and λ_n satisfies $\cosh(\lambda)\cos(\lambda) = 1$ and m, n are integers.

Using the orthogonal property of the mode shape functions, we can convert the partial differential equations of the distributed system into an infinite set of ordinary differential equations.

$$KW_P(t) + M_I \ddot{W}_P(t) = F_P \tag{5}$$

where

$K = D \cdot$

$$\begin{bmatrix} \int_\sigma \left(\frac{\partial^4}{\partial x^4} + 2\frac{\partial^4}{\partial x^2\,\partial y^2} + \frac{\partial^4}{\partial y^4}\right) S_1^2 \,\mathrm{d}\sigma & \cdots & 2\int_\sigma \frac{\partial^4 S_l S_1}{\partial x^2\,\partial y^2}\,\mathrm{d}\sigma \\ \vdots & \ddots & \vdots \\ \textit{Symmetric} & \cdots & \int_\sigma \left(\frac{\partial^4}{\partial x^4} + 2\frac{\partial^4}{\partial x^2\,\partial y^2} + \frac{\partial^4}{\partial y^4}\right) S_l^2 \,\mathrm{d}\sigma \end{bmatrix}_{l\times l}$$

is a real symmetric matrix, $M_I = \rho_s hab \cdot I_{l\times l}$ is a diagonal matrix, I is the unit matrix and $F_P(t) = [\int_\sigma S_1 P_e(x, y, t)\,\mathrm{d}\sigma, \ldots, \int_\sigma S_l P_e(x, y, t)\,\mathrm{d}\sigma]^{\mathrm{T}}_{l\times 1}$ is the forcing term converted from the external force.

2.2. TRANSMISSION OF AN INCIDENT PLANE WAVE

Now, we consider an acoustic plane wave P_{in} incident to the plate

$$P_{in}(\mathbf{r}, t) = P_0 \exp(-i\mathbf{k}\cdot\mathbf{r} + i\omega t) \tag{6}$$

where

$\mathbf{k} = k_x\mathbf{i} + k_y\mathbf{j} + k_z\mathbf{k} = k\sin\theta\cos\phi\mathbf{i} + k\sin\theta\sin\phi\mathbf{j} + k\sin\phi\mathbf{k}$, $\mathbf{r} = x\mathbf{i} + y\mathbf{j} + z\mathbf{k}$

and $k = \omega/C_0$ is the acoustic wavenumber.

If we assume that the plate is a rigid wall than the pressure field exciting the plate into motion will be twice the incident pressure, and we can derive the plate forced response to the incident acoustic wave.

The transmitted sound wave due to the plate motion is assumed to propagate in the semi-infinite space. If the distance R from the origin to the field point is long enough compared with the wave length λ, the far field of the transmitted sound $P_{rad}(t)$ can be computed from the structural response by using the Rayleigh integral:

$$P_{rad}(\mathbf{R}, t) = \frac{\rho_a}{2\pi}\int_\sigma \ddot{w}(\sigma, t)\frac{\exp(-ik|\mathbf{R} - \mathbf{r}_\sigma|)}{|\mathbf{R} - \mathbf{r}_\sigma|}\,\mathrm{d}\sigma.$$

The pressure resulting from the acceleration distribution

$$\ddot{w}(\sigma, t) = S_P(\sigma)^{\mathrm{T}}\ddot{W}_P(t)$$

associated with the Pth spatial function on the structure can be written as [5]

$$P_{rad}(\mathbf{R}, t) = \frac{\rho_a\exp(-ikR)}{2\pi R}\int_\sigma S_P(\sigma)^{\mathrm{T}}\exp(i\mathbf{k}\cdot\mathbf{r}_\sigma)\,\mathrm{d}\sigma\cdot\ddot{W}_P(t)$$

$$= \frac{\rho_a\exp(-ikR)}{2\pi R}\hat{H}^{\mathrm{T}}\cdot\ddot{\mathbf{W}}_P(t) \tag{7}$$

where

$$\hat{H} = i\omega\int_\sigma S_P(\sigma)^{\mathrm{T}}\exp(i\mathbf{k}\cdot\mathbf{r}_\sigma)\,\mathrm{d}\sigma.$$

By the acoustic far field assumption, the proportionality constant (between pressure and velocity) will be the characteristic impedance $\rho_a C_0$. This relationship holds for instantaneous signals as well as steady-state signals.

Using the real-valued pressure and fixing R, the intensity I radiated into the far field in direction (θ, ϕ) is

$$I(\theta, \phi) = \frac{|P|^2}{\rho_a C_0}.$$

The total radiated power can be obtained from the integration of sound intensity I over a hemisphere of radius R in the far field. Thus the power is expressed as

$$\Pi = \int_0^{2\pi}\int_0^{\pi/2} I(\theta, \phi)R^2\sin\theta\,\mathrm{d}\theta\,\mathrm{d}\phi$$

$$= \ddot{W}_P(t)^{\mathrm{T}*}\cdot M\cdot\ddot{W}_P(t) \tag{8}$$

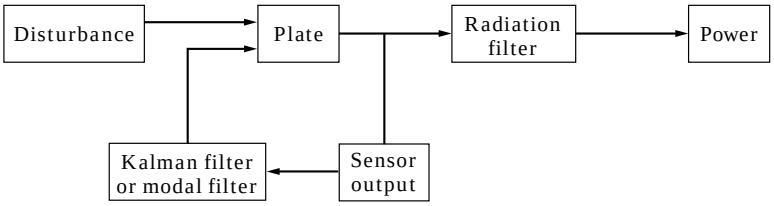

Figure 2. The block diagram of the control system.

where

$$\bar{M} = \frac{\rho_a}{4\pi^2 C_0} \int_0^{2\pi} \int_0^{\pi/2} \hat{H}^* \cdot \hat{H}^{\mathrm{T}} \sin\theta \, \mathrm{d}\theta \, \mathrm{d}\phi,$$

* means the complex conjugate and $\bar{M}$ is real, symmetric and non-negative matrix. Note that the matrix $\bar{M}$ has explicit physical significance, defining the relationship between structural modal acceleration levels and radiated acoustic power. The diagonal terms of the matrix $\bar{M}$ are relevant to the value of the power that results from the vibration of a single, isolated structural mode, and the off-diagonal terms are relevant to the modification to this value caused by the coexistence of the other structural modes. In general, $\bar{M}$ will be of normal rank P. For certain degenerate cases, it may happen that $\bar{M}$ will be of normal rank $r < P$. This is also discovered by Baumann [6].

2.3. CONTROL DESIGN

A controller was designed using modal space for the structural dynamics. The traditional view of feedforward controlled system is of "active cancellation" where the modes of the structure excited by the "primary" disturbance input are cancelled by the "secondary" control input of appropriate magnitude and phase driving the same structural modes. This view arises from the superposition theorem of the system response. However, recent work has shown that the feedforward controlled system responds effectively with a new set of eigenfunctions and eigenvalues to the disturbance input [7]. The controlled resonant frequencies and associated eigenfunctions are functions of the selected control actuators and independent of the disturbance input. Thus, the design approach is based on

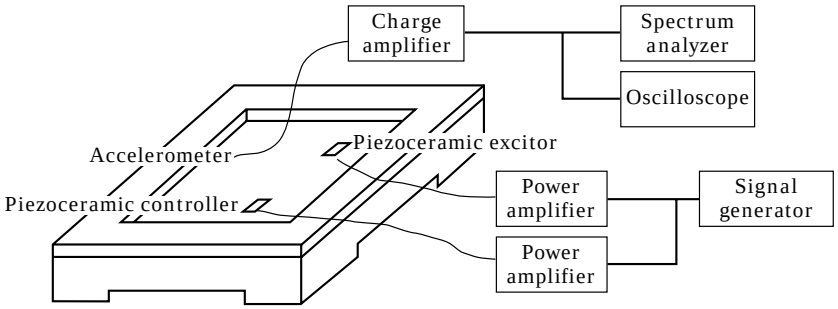

Figure 3. The arrangement of the plate with the measuring system.

finding the configuration of the actuators such that the controlled structure will respond to the weakest set of modal radiators.

The effect of the square piezoceramic patch, which has been shown in the previous research [4], can be treated as four point moments concentrated on the midpoint of four edges. The point moment m_0 generated at the midpoint of the four edges is related to the external voltage $V(t)$ by coupling constant [4] κ_0:

$$m_0 = \kappa_0 V(t). \tag{9}$$

Since this model has been shown to be a good approximation of the piezoelectric actuator when the dimension of the square ceramic is far less than that of the plate. The resulting displacement of the plate under the excitation of the piezoelectric actuator is obtained as [4]

$$\begin{aligned} w(x, y, t) = \sum_m \sum_n \frac{\kappa_0 V(t) X_m(x) Y_n(y)}{M_I(\omega_{mn}^2(1 + i\eta) - \omega^2)} \Bigg[& Y_n(\zeta) \cdot \frac{\partial X_m(\xi)}{\partial \xi}\Bigg|_{\substack{\xi = \xi_0 - l_p/2 \\ \zeta = \zeta_0}} \\ & - Y_n(\zeta) \cdot \frac{\partial X_m(\xi)}{\partial \xi}\Bigg|_{\substack{\xi = \xi_0 + l_p/2 \\ \zeta = \zeta_0}} \\ & + X_m(\xi) \cdot \frac{\partial Y_n(\zeta)}{\partial \zeta}\Bigg|_{\substack{\xi = \xi_0 \\ \zeta = \zeta_0 - l_p/2}} \\ & - X_m(\xi) \cdot \frac{\partial Y_n(\zeta)}{\partial \zeta}\Bigg|_{\substack{\xi = \xi_0 \\ \zeta = \zeta_0 + l_p/2}} \Bigg] \end{aligned} \tag{10}$$

where ω_{mn} is the natural frequency of (m, n) mode, η is the loss factor, l_p is the length of the ceramic and (ξ_0, ζ_0) is the coordinate of the centre of actuator.

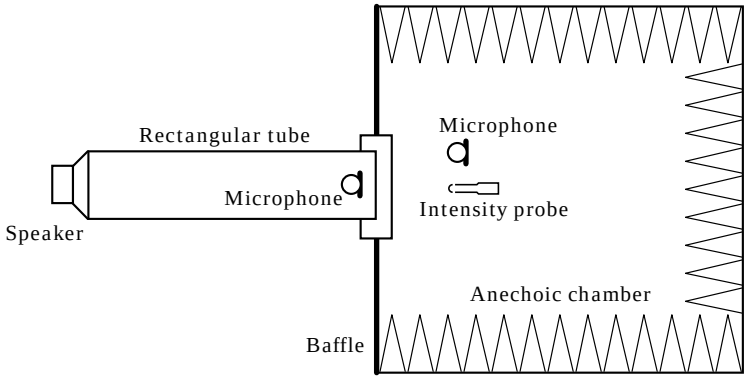

Figure 4. The setup of the rectangular waveguide and the anechoic chamber.

TABLE 1

Comparison of natural frequencies

Mode		1	2	3	4	5	6	7	8	9	10
Frequency (Hz)	Calculated	106·93	218·09	218·09	321·58	390·99	392·85	490·36	490·36	625·57	625·57
	Experimental	106·00	216·70	216·70	318·30	389·25	389·25	487·50	487·50	622·14	622·14
	Ritz method	105·70	215·70	215·70	318·00	386·60	388·50	484·80	484·80	618·60	618·60

TABLE 2

Calculated and measured transmitted sound power in the anechoic chamber

Frequency (Hz)	Incidence sound pressure (dB)	Incidence sound power (dB)	Transmission sound power (dB)	
			Calculated	Measured
105	95·85	87·72	71·78	80·16
390	101·25	93·12	73·92	80·32

TABLE 3

Natural frequencies of controlled system

Mode	1	2	3	4	5	6	7
Controlled natural frequency (Hz)	118·00	218·09	222·42	304·78	321·60	390·00	488·89

Now, we introduce the effect of the actuator and the incident pressure to equation (5), and it can be written as:

$$\ddot{W}_P(t) = -M_I^{-1}KW_P(t) + M_I^{-1}Bu(t) + M_I^{-1}Lv(t) \tag{11}$$

where B is the location matrix of the actuators; $u(t) \in R^m$ is a vector of the actuator inputs that can be used to control the structure and L is the location matrix of the disturbance input; $v(t)$ is a vector of the disturbance input.

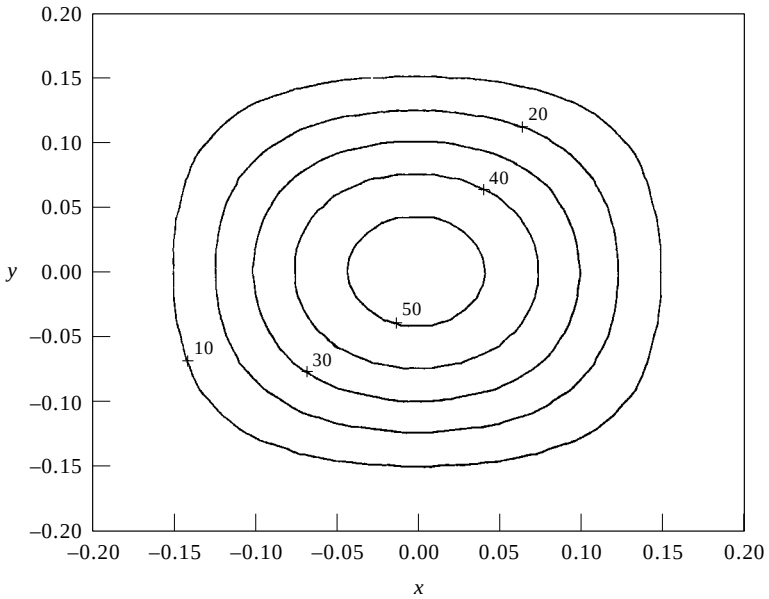

Figure 5. The displacement contour of the plate subject to 106·93 Hz plane-wave normal incidence before control (unit: μm).

By introducing equation (11) to equation (8) and assuming the disturbance input is unknown, we choose the cost function J as follows

$$J = W_P(t)^{\mathrm{T}*} \cdot \tilde{A} \cdot W_P(t) + W_P(t)^{\mathrm{T}*} \cdot \tilde{B} \cdot u(t) + u(t)^{\mathrm{T}*} \cdot \tilde{B}^{\mathrm{T}*} \cdot W_P(t) + u(t)^{\mathrm{T}*} \cdot \tilde{C} \cdot u(t) + \beta u(t)^{\mathrm{T}*} \cdot u(t) \tag{12}$$

where

$$\tilde{A} = (-M_I^{-1}K)^H \cdot \bar{M} \cdot (-M_I^{-1}K),$$
$$\tilde{B} = (-M_I^{-1}K)^H \cdot \bar{M} \cdot (-M_I^{-1}B),$$
$$\tilde{C} = (-M_I^{-1}B)^H \cdot \bar{M} \cdot (-M_I^{-1}B),$$

and β is a constant which limits the amount of control energy that can be applied in a given time interval. As β approaches zero, the control energy is less constrained and the cointrol effect is better.

The optimal control is a time-invariant modal amplitude feedback of the form

$$u_{OPT}(t) = G_z W_P(t) = -(\tilde{C} + \beta \cdot I)^{-1} \cdot \tilde{B}^{\mathrm{T}*} \cdot W_P(t). \tag{13}$$

If the full modal amplitude is not available for feedback, the problem is how to estimate the modal amplitude by a finite number of sensors. This can be accomplished by a Kalman filter or a modal filter [8] and the estimates are used in the feedback control law. Figure 2 shows the overall system (the plate/control system) block diagram.

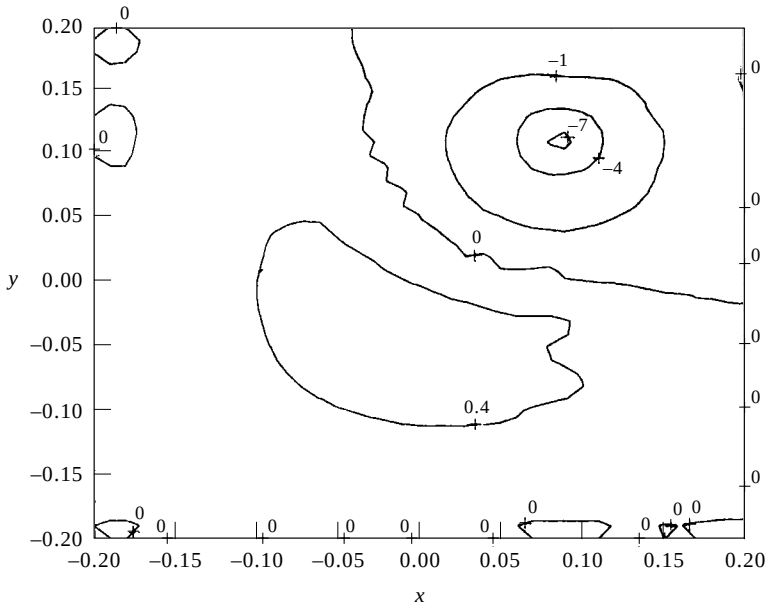

Figure 6. The displacement contour of the plate subject to 106·93 Hz plane-wave normal incidence after control (unit: μm).

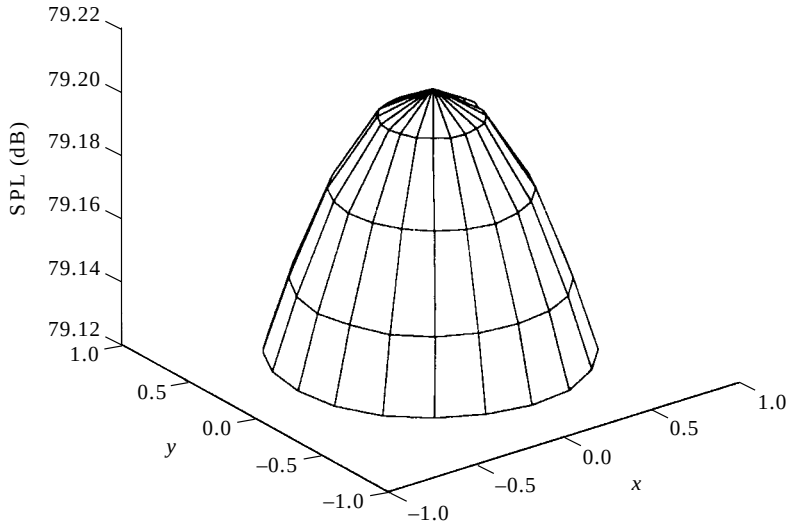

Figure 7. The SPL at half sphere surface of radius 1·0 m for the plate subject to 106·93 Hz plane-wave normal incidence before control.

3. RESULTS AND DISCUSSION

The dimension and material constants of the clamped square plate are chosen as follows: $a = b = 0{\cdot}4$ m, thickness $h = 2$ mm, density $\rho_s = 7099$ kg/m^3, Young's modules $E = 190 \times 10^9$ N/m^2, Poisson ratio $v = 0{\cdot}3$, and loss factor $\eta = 0{\cdot}0045$. The density of the air, ρ_a, and sound speed, C_0, are 1·21 kg/m^3 and 344 m/s respectively. Each piezoceramic patch measured 25 mm × 25 mm × 1 mm and weighed 6·3 g. The centers of the No. 1 and No. 2 piezoceramics are located at $(-11{\cdot}25, 8{\cdot}75)$ cm and $(-8{\cdot}75, -11{\cdot}15)$ cm respectively. For measuring the plate

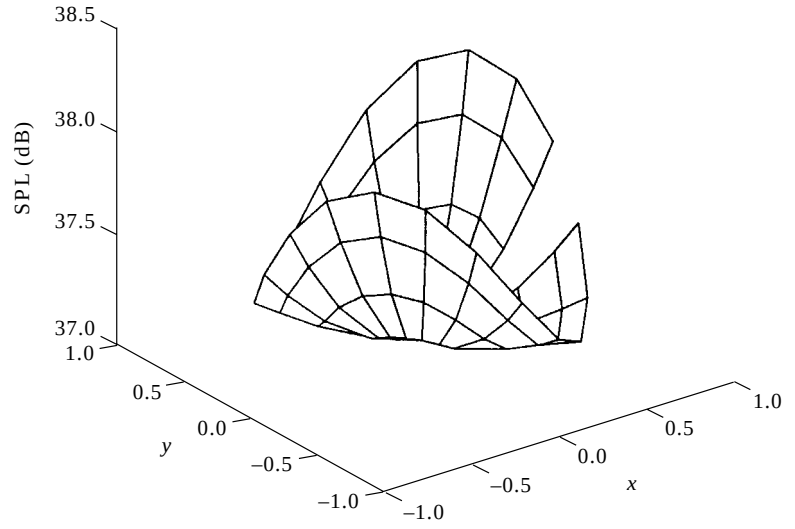

Figure 8. The SPL at half sphere surface of radius 1·0 m for the plate subject to 106·93 Hz plane-wave normal incidence after control.

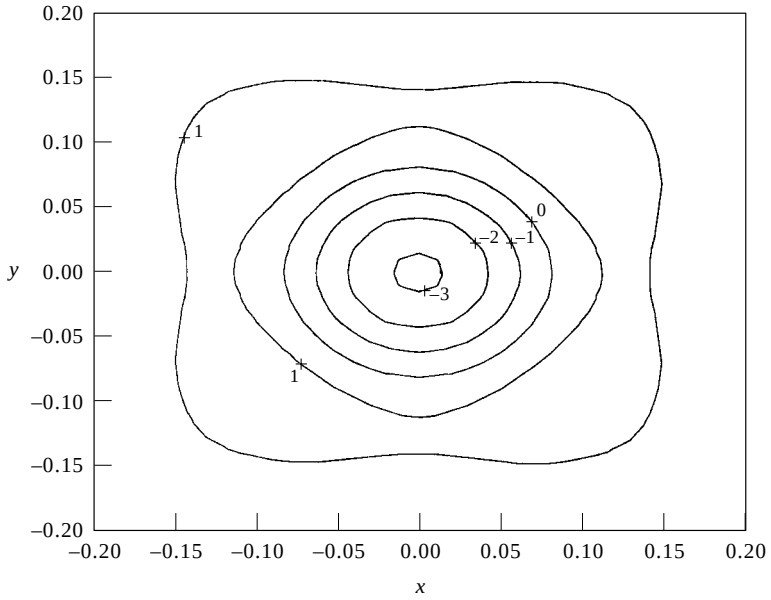

Figure 9. The displacement contour of the plate subject to 390·99 Hz plane-wave normal incidence before control (unit: μm).

responses, one of the piezoceramic patches was used as an actuator to excite the plate and an accelerometer (B&K 4393), weighing 2·2 g, was used as an acceleration sensor. Figure 3 shows the arrangement of the plate and the response measuring system and Table 1 lists the calculated and experimental frequencies.

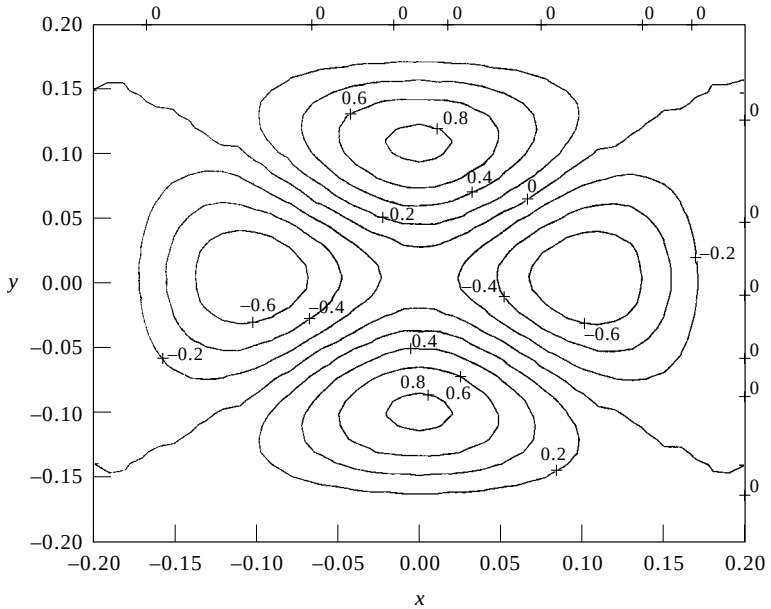

Figure 10. The displacement contour of the plate subject to 390·99 Hz plane-wave normal incidence before control (unit: μm).

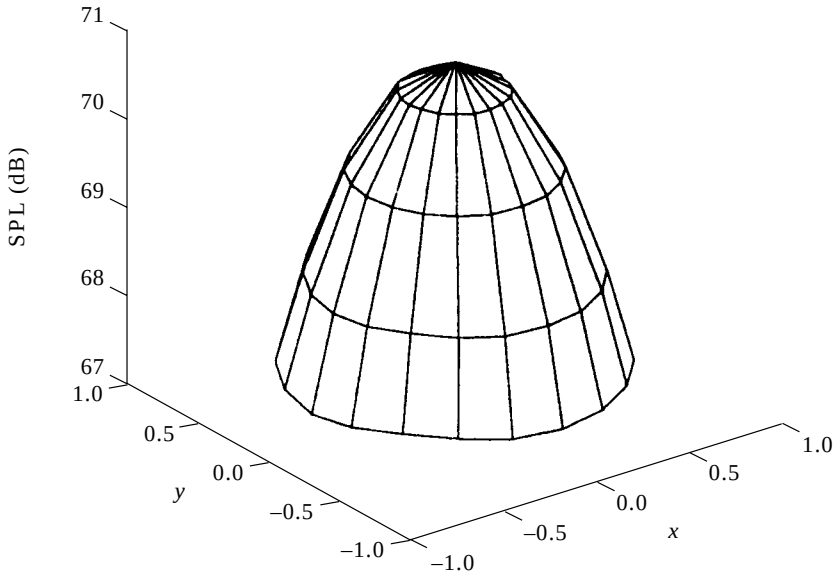

Figure 11. The SPL at half sphere surface of radius 1·0 m for the plate subject to 390·99 Hz plane-wave normal incidence before control.

The arrangement of the clamped plate described above was baffled and placed on the opening of the anechoic chamber (Figure 4). A 0·4 m × 0·4 m × 1·2 m rectangular wave guide was attached to the frame of the plate perpendicularly on the other side of the plate. A microphone was placed in the pipe 0·2 m in front of the plate. A microphone and a sound intensity probe were also placed 0·2 m from the rear of the plate in the anechoic chamber. Harmonic disturbance,

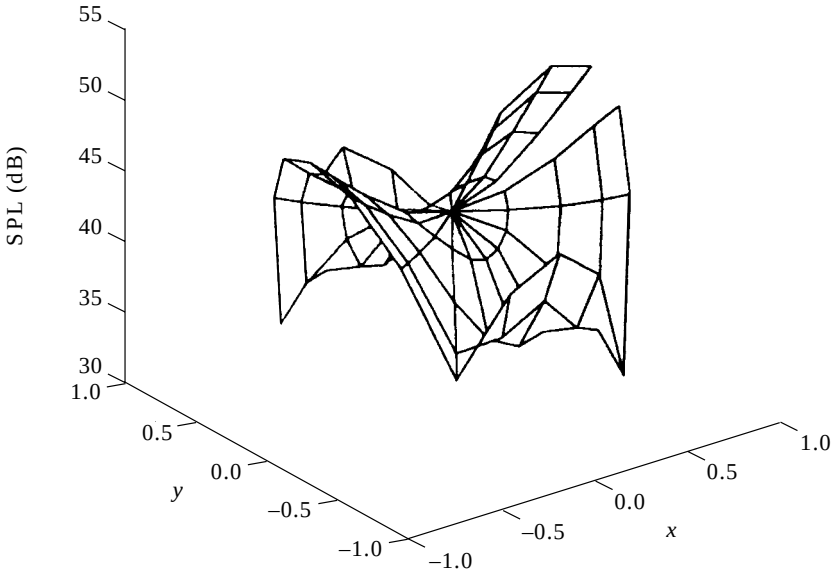

Figure 12. The SPL at half sphere surface of radius 1·0 m for the plate subject to 390·99 Hz plane-wave normal incidence after control.

TABLE 4

Transmitted acoustic power before and after control (*re*: 10^{-12} *W*)

Frequency (Hz)		106·93	390·99
Incidence sound power (dB)		85·85	85·85
Transmission sound power (dB) without control		84·90	70·47
Transmission sound power (dB)	Controlled by PZT 1	50·56	58·54
	Controlled by PZT 1 and 2	47·74	40·87

generated using a loud speaker, mounted on the other end of the pipe, was applied onto the plate as the normal incident wave. The microphone in the pipe was used for measuring the incident sound pressure. The microphone and sound intensity probe in the anechoic chamber were used to measure the transmitted sound pressure and sound intensity respectively. Table 2 shows the comparison of the calculated and measured transmitted sound power.

Due to plane wave normal incidence, only the (odd, odd) eigen modes can be excited. Table 3 shows the new natural frequencies of the controlled system when the plate is excited at 106·93 Hz and controlled by the No. 1 actuator. The rank of the system dynamic matrix after control is reduced by 1, i.e., the controller reduces the dynamic degrees of freedom of the system by 1 and makes the structural response a linear contribution of weak radiating mode. It can be also seen that the resonant frequencies of the system were pushed away from the spectrum of the disturbance input. Figures 5 and 6 show the displacement contour diagrams of the plate subjected to plane wave normal incidence at 106·93 Hz without control and controlled by No. 1 actuator respectively. The amplitude of the displacement is significantly reduced and the shape of the contour is altered. Figures 7 and 8 show the corresponding sound pressure level (SPL) at the half sphere surface of radius $R = 1{\cdot}0$ m. Figures 9 and 10 show the displacement contour diagrams of the plate subjected to plane wave normal incidence at 390·90 Hz without control and controlled by No. 1 actuator respectively. It can be seen that after control the plate is shifted to the mode with low radiation efficiency and the displacement amplitude is substantially reduced. The global sound pressure level is also reduced after control (Figures 11 and 12). Table 4 shows the comparison of acoustic power before and after control when one or two actuators are employed. The reductions of plate displacement, sound pressure level and acoustic power are further increased as the number of the actuator increases.

4. CONCLUSIONS

In this paper, a technique using point structural sensors has been developed for the prediction of acoustic power transmitted through thin plate. The experimental verification has been accomplished in the anechoic chamber equipped with a rectangular wave guide. Details are sketched for a pure tone active control of sound transmission through the plate. By changing the system to a weaker radiator

via the control strategy, the reduction of transmitted acoustic power can be reached at about 30–40 dB by one or two piezoelectric actuators. The global sound pressure level is also reduced at about 20–30 dB. The results show that for a low to middle frequency range, substantial reductions in acoustic power can be achieved with one or two actuators.

REFERENCES

1. C. R. Fuller 1980 *Journal of Sound and Vibration* **136**(1), 1–15. Active control of sound transmission/radiation from elastic plates by vibration inputs: I. Analysis.
2. C. R. Fuller 1992 *Journal of Sound and Vibration* **153**(3), 387–402. Active control of sound transmission/radiation from elastic plates by vibration inputs: II. Experiments.
3. S. Akishita and Y. Mitani 1994 *Journal of Intelligent Material Systems and Structures* **5**, 371–378. Sound transmission control through rectangular plate by using piezoelectric ceramics as actuators and sensors.
4. C. C. Sung and J. T. Jan 1997 *Journal of Sound and Vibration* **207**(3), 301–317. The response of and sound power radiated by a clamped rectangular plate.
5. C. C. Sung and J. T. Jan 1997 *Journal of the Acoustical Society of America* **102**(1), 370–381. Active control of structurally radiated sound from plate.
6. M . C. Junger and D. Feit *Sound*, *Structures*, *and their Interaction*, p. 89.
7. W. T. Baumann 1991 *Journal of the Acoustical Society of America* **90**(6), 3202–3208. Active suppression of acoustic radiation from impusively excited structures.
8. R. A. Burdisso and C. R. Fuller 1992 *Journal of Sound and Vibration* **153**, 437–452. Theory of feedforward controlled system eigenproperties.
9. L. Meirovitch and H. Baruh 1983 *Journal of Guidance* **6**(1), 20–25. Robustness of the independent modal-space control method.